Report 2

Forward Seismic Modeling Using 1D Convolution with Weak Contrast Approximation of Reflectivity *

* CIPR-PETROMAKS Project Report, 2009.

Abul Fahimuddin

Center for Integrated Petroleum Research (CIPR)
University of Bergen, Norway

Forward Seismic Modeling Using 1D Convolution with Weak Contrast Approximation of Reflectivity

Introduction

In order to compare the field observation data, e.g., well production information or time-lapse seismic data, with simulated data, one has to perform forward modeling at different stages of reservoir modeling work flow. An example of forward modeling, in the geophysical exploration context, is the process of generating synthetic seismograms for seismic modeling. It involves three steps: reservoir simulation, petro-elastic modeling (PEM) and calculation of seismic traces for a given time window. In this process, at first, reservoir parameters, e.g., porosity, pressure and saturation are converted to seismic parameters, e.g., saturated P-wave velocity or density of fluid mixture by using the rock physics models. Then, synthetic seismic sections are calculated based on these seismic parameters. Numerous methods for seismic modeling exist including the finite difference method, reflectivity method and a simple convolution-based method. For simplicity, we restrict ourselves to primary waves and post-stack data, and therefore use simple convolution-based forward modeling [12].

A synthetic seismic trace represents the combined reflection response of the layered ground (i.e. the output for a spike input) and the recording system to a seismic pulse. A synthetic seismogram or time series, $S(x,t)$ may be considered as the assumed source function $\omega(t)$, convolved with a reflectivity function $r(x,t)$, representing the contrasts in acoustic impedance in the layered model, and $S(x,t)$ can be expressed as

$$S(x,t) = \omega(t) \otimes r(x,t), \tag{1}$$

where x is the lateral location and t is the two-way vertical seismic travel time. This process is also called 1D convolution. For time-lapse seismic modeling, it is assumed that the wavelet does not change with production time. The reflection coefficients are a function of seismic velocity and density and are therefore dependent on the production time step. Eqn. (1) is used to generate the synthetic seismic response for different production time steps. However, in general the geological structure in both overburden and reservoir may be very complex. Hence, an accurate modeling is required, and typically finite-difference modeling (FDM) [14] or ray-tracing methods [7] are applied.

Weak Contrast Approximation of Reflection Coefficients

In a marine seismic survey, an air-gun array behind the seismic vessel is fired, generating waves that propagate in the water until they reach the subsurface. The hydrophones on the seismic streamers register the amplitudes of the reflected waves that give account of the change of the properties of the medium and the portions of the wave which are reflected back to the surface. The result is a set of reflected wave amplitudes, $d^j_{s_k,\theta_l}$, at different locations, $j \in \{1,2,\cdots,n_{xy}\}$, as a function of discretized seismic reflection travel time, s_k, $k \in \{1,2,\cdots,S\}$ and reflection angles, θ_l, $l \in \{1,2,\cdots,n_\theta\}$. The seismic trace refers to the set of reflected amplitudes along a vertical profile, $\mathbf{z}_i \in \mathbf{R}^z$ with z is the reservoir dimension in the depth direction, for

different reflection angles at the lattice nodes j can be represented by the vector

$$\mathbf{d}^j = \left[d^j_{s_1,\theta_1}, \cdots, d^j_{s_S,\theta_1}, \cdots, d^j_{s_1,\theta_{n_\theta}}, \cdots, d^j_{s_S,\theta_{n_\theta}} \right]^T \in \mathbf{R}^{n_\theta \cdot S \times 1} \tag{2}$$

where n_{xy} is the total number of reservoir grid cells in X and Y directions; n_θ number of different incidence angles and S corresponds to the total two-way travel time. In this section, we are interested to implement a forward model connecting a reservoir, $\mathbf{r}_t$ to the observed seismic amplitude data, $\mathbf{d}^j_t$ at certain time steps, $t \in \mathbf{T}_d$.

The forward modeling of a seismic time-angle gather is based on the matrix-vector formulation in Buland and Omre [5]. The forward model is linear that uses weak contrast expressions for reflection coefficients by Aki and Richards [1]. An isotropic, elastic medium is completely described, according to Sheriff and Geldart [13], by three elastic parameters, such as P-wave velocity, S-wave velocity and density, $\{\mathbf{V}_P(\mathbf{x}, s), \mathbf{V}_S(\mathbf{x}, s)$ and $\boldsymbol{\rho}(\mathbf{x}, s)\}$. The single-interface reflection coefficient in the Aki and Richards formulation can be extended to a time-continuous reflectivity function r_{PP}, as

$$\begin{aligned} r_{PP}(s,\theta) = \mathbf{a}_{V_p}(s,\theta)\frac{1}{\partial s}\ln \mathbf{V}_p(s) + \mathbf{a}_{V_S}(s,\theta)\frac{1}{\partial s}\ln \mathbf{V}_S(s) \\ + \mathbf{a}_\rho(s,\theta)\frac{1}{\partial s}\ln \boldsymbol{\rho}(s), \end{aligned} \tag{3}$$

where $\mathbf{a}_{V_P}$, $\mathbf{a}_{V_S}$ and $\mathbf{a}_\rho$ are the generalizations of the reflection coefficients with time dependent velocities $\bar{\mathbf{V}}_P(s)$ and $\bar{\mathbf{V}}_S(s)$. We assume that $\bar{\mathbf{V}}_P(s)$ and $\bar{\mathbf{V}}_S(s)$ can be represented by constant or slowly varying known background model, such that $\bar{\mathbf{V}}_P(s)$ and $\bar{\mathbf{V}}_S(s)$ are the average or moving average of $\mathbf{V}_P$ and $\mathbf{V}_S$ in a relatively small time window.

The material parameters $\mathbf{V}_P(s)$, $\mathbf{V}_S(s)$ and $\boldsymbol{\rho}(s)$ are a priori assumed to be log-Gaussian, which implies that the parameters are restricted to take positive values [6]. This assumption is required for later analytical treatment due to Eqn. (3). The logarithm of these material parameters defines a continuous Gaussian vector field

$$m(s) = \left[\ln \mathbf{V}_P(s) \ln \mathbf{V}_S(s) \ln \boldsymbol{\rho}(s) \right]^T. \tag{4}$$

The continuous form of the Gaussian field $m(s)$, makes it possible to give a proper definition of the time differentiated Gaussian field $m(s)'$, which can be expressed as

$$m(s)' = \left[\frac{1}{\partial s}\ln \mathbf{V}_P(s) \frac{1}{\partial s}\ln \mathbf{V}_S(s) \frac{1}{\partial s}\ln \boldsymbol{\rho}(s) \right]^T. \tag{5}$$

The next step is to formulate a discrete version of the reflectivity function, $r_{PP}(s,\theta)$ for a given time interval and a set of reflection angles in the matrix-vector form. For each discretized seismic trace $\mathbf{d}^j$, $j \in \{1, 2, \cdots, n_{xy}\}$, we can write:

$$\mathbf{r}^j = \mathbf{A}_j \mathbf{m}'_j = \mathbf{A}\mathbf{D}m, \tag{6}$$

with the matrices defined as:

$$\mathbf{A} = \begin{bmatrix} \mathbf{A}_{V_p}(\theta_1) & \mathbf{A}_{V_s}(\theta_1) & \mathbf{A}_\rho(\theta_1) \\ \vdots & \vdots & \vdots \\ \mathbf{A}_{V_P}(\theta_{n_\theta}) & \mathbf{A}_{V_s}(\theta_{n_\theta}) & \mathbf{A}_\rho(\theta_{n_\theta}) \end{bmatrix},$$

, where $\mathbf{A}_{V_p}(\theta_i)$, $\mathbf{A}_{V_s}(\theta_i)$ and $\mathbf{A}_{\rho}(\theta_i)$ are $(n_m/3) \times (n_m/3)$ diagonal matrices containing discrete time samples of $\mathbf{a}_{V_p}(s, \theta_i)$, $\mathbf{a}_{V_p}(s, \theta_i)$ and $\mathbf{a}_{\rho}(s, \theta_i)$, respectively; n_θ is the number of reflection angles and n_m is the dimension of $m(s)$. Here, $\mathbf{m}'$ denotes the discrete version of the differentiated field of the layer properties. As differentiation is a linear operation, we can write that $\mathbf{m}' = \mathbf{D}m$ with $\mathbf{D}$ holding the relative contrasts of the differentiated layer model.

Wavelet Discretization & Convolution

The seismic observations are connected to the reflection coefficients r_{PP}, through the convolution model described by Dobrin and Savit [8] as

$$\mathbf{d}(\theta, s) \;=\; \int \omega_\theta(s-u)\, r_{PP}(\theta, u)\, \mathrm{d}u + \epsilon(\theta, s), \tag{7}$$

where $\omega_\theta(s-u)$, is a seismic wavelet dependent on the angle of incidence, θ, u is a slack variable and ϵ is the error term. Ideally, the Eqn. (7) simulates the response to a delta function or a spike-like source because only such a wavelet would enable us to identify individual interfaces [12]. In practice, however such an ideal source-time function is impossible to achieve. As the Earth acts as a filter in which high frequencies are attenuated as the energy propagates through the earth, the shape of the wavelet changes with time. For all practical purposes, a wavelet is assumed to be stationary and band-limited; often an average wavelet is estimated from seismic data. In seismic data processing, the wavelet is usually removed, and a simpler, so-called zero-phase wavelet is convolved. The most common zero-phase wavelet is a Ricker wavelet [10] described by the equation

$$f(t) \;=\; (1 - 2\pi^2\omega_{max}^2 t^2)\exp(-\pi^2\omega_{max}^2 t^2), \tag{8}$$

where $f(t)$, is the amplitude of the wavelet at time t and ω_{max} is the peak frequency of the wavelet. In the discretized framework for convolution with reflection coefficient, one needs to perform discretization of the evaluated Ricker wavelet along a trace. For seismic exploration purposes, it is common to use a band-limited Ricker wavelet with 25-40 Hz peak frequency.

In the frequency domain, convolution is equivalent to multiplication and hence, according to Buland and Omre [5], the integral expression for convolution can be further discretized such that

$$\mathbf{d}^j \;=\; \mathbf{W}\,\mathbf{r}^j \;+\; \boldsymbol{\epsilon}_\omega, \tag{9}$$

where $\boldsymbol{\epsilon}_\omega = [\epsilon(\theta_1, s_1), \cdots, \epsilon(\theta_1, s_S), \cdots, \epsilon(\theta_{n_\theta}, s_1), \cdots, \epsilon(\theta_{n_\theta}, s_S)]^T$ with the same dimension of $\mathbf{d}^j$ and a block diagonal matrix, $\mathbf{W} \in \mathbf{R}^{n_\theta \cdot S \times n_\theta \cdot S}$ with diagonal elements

$$\mathbf{W}_\kappa \;=\; \begin{bmatrix} \mathbf{w}_1 & 0 & \cdots & 0 \\ 0 & \mathbf{w}_\omega & \ddots & 0 \\ \vdots & \ddots & \ddots & 0 \\ 0 & \cdots & 0 & \mathbf{w}_S \end{bmatrix} \in \mathbf{R}^{S \times S},\; \kappa \in \{1, 2, \cdots, n_\theta\} \tag{10}$$

with the discretized diagonal element component, $\mathbf{w}_m$ which depends on the choice of the wavelet sampling frequency [11].

Normally, the velocity or reflection coefficients calculated from the reservoir simulation model are depth converted and sampled into a regular time grid before performing the convolution. Here we have applied a different procedure, where all the calculations, including the convolution, are performed in dept This will of course

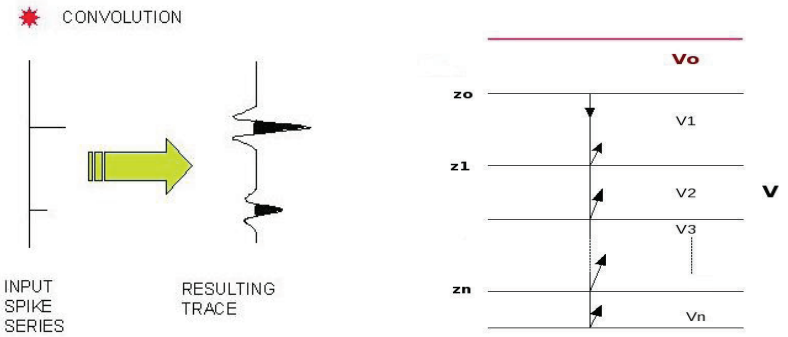

(a) Ricker wavelet (b) Vertical reflected ray paths

Figure 1: Ricker wavelet and time-to-depth relationship.

not be possible in a real case. However, in this way we are able to generate a synthetic problem where these errors are minimized, allowing us to focus on the differences using inverted and not-inverted data in the history-matching procedure. In addition, it simplifies calculations. Note that if the layer thicknesses are constant, and applying the common assumption that the velocity variations within the reservoir section are small ($\Delta V_i \ll V_i \approx V$), the time-depth relation for a normal incident wave simplifies to

$$t_i = 2\left[(\frac{1}{V_o} - \frac{1}{V_1})z_0 \; + \; (\frac{1}{V_1} - \frac{1}{V_2})z_1 + \cdots + \; \frac{z_i}{V_i}\right] \approx 2\left[\frac{z_0}{V_o} + \frac{z_i - z_0}{V}\right], \; i = 1, \cdots, n. \quad (11)$$

This model assumes each layer to be characterized by an interval velocity V_i, and with z_i, as the thickness of such interval and V_o is the over-burden velocity (see, Fig. 1b). Here the horizontal layer interval velocity may be averaged over several depth intervals to yield a time-average velocity V. That is, our approach is exact within this approximation provided the sampling interval $\Delta t = 2\overline{\Delta z}/V$, where $\overline{\Delta z}$ is the average layer thickness. The breadth (distance between each of the two side lobes) of a normal Ricker wavelet in time is given by $B_t = \frac{\sqrt{6}}{\pi\omega_{max}}$. From the discretized version of Eq. (7), it follows that the average breadth of the wavelet (in depth) in our approach is equal to $B_d = \frac{10\sqrt{6}}{\pi}\overline{\Delta z}$. Thus, the corresponding average time-wavelet frequency in our approach, is given (in Hz) by

$$f = \frac{\sqrt{6}}{\pi B_t} \; = \; \frac{\sqrt{6}}{\pi}\frac{V}{2B_d} = \frac{V}{20\overline{\Delta z}}. \quad (12)$$

If we consider an average velocity V= 2500m/s, and an average cell thickness $\overline{\Delta z}$= 3.9 m, the "effective" wavelet frequency corresponding to a time frequency is close

to 30Hz. The corresponding sampling interval in time becomes approximately 3 milliseconds. Thus, sampling of wavelet in depth in our case is a reasonable approximation for a synthetic case.

Discretized Seismic Amplitude in Depth

The seismic data are represented as a convolutional model, and the seismic time-angle, $\mathbf{d}_{obs}$ at location x, can be written in vector-matrix form as

$$\mathbf{d}_{obs} = \mathbf{W}\,\mathbf{r} + \mathbf{e}, \tag{13}$$

where $\mathbf{e}$ is an n_d-dimensional error vector, and $\mathbf{W}$ is a block-diagonal matrix containing one wavelet for each reflection angle sampled in depth. The sampling of the wavelet, in this case, is equal to the sampling of the seismic data. In an expanded matrix-vector form, this relationship can be written as:

$$\begin{bmatrix} \mathbf{d}_{obs}(\theta_1) \\ \vdots \\ \mathbf{d}_{obs}(\theta_{n_\theta}) \end{bmatrix} = \begin{bmatrix} \mathbf{W}(\theta_1) & & \\ & \ddots & \\ & & \mathbf{W}(\theta_{n_\theta}) \end{bmatrix} \times \begin{bmatrix} \mathbf{r}(\theta_1) \\ \vdots \\ \mathbf{r}(\theta_{n_\theta}) \end{bmatrix} + \begin{bmatrix} \boldsymbol{e}(\theta_1) \\ \vdots \\ \boldsymbol{e}(\theta_{n_\theta}) \end{bmatrix}. \tag{14}$$

The seismic time-angle gather at location $\mathbf{s}$ can now be written in a compact formulation as

$$\mathbf{d}_{obs} = \mathbf{G}\,m + \mathbf{e} = \mathbf{WAD}\,m + \mathbf{e}, \tag{15}$$

where the $n_d \times n_m$-dimensional matrix, $\mathbf{G} = \mathbf{WAD}$, is a linear modeling operator for the seismic time-angle gather at location $\mathbf{x}$. Following the approach proposed by Bachrach [3], it is possible to link the elastic parameters, $\mathbf{V}_P$, $\mathbf{V}_S$ and $\boldsymbol{\rho}$ with the reservoir properties, e.g., porosity, ϕ and water saturation, s_w through a non-linear function, $\mathbf{g} : \mathbf{R}^3 \rightarrow \mathbf{R}^3$, by using the Biot-Gassmann theory [9] and the empirical results of Batzle and Wang [4].

Example of Seismic Modeling

The reservoir simulation model is a black-oil model of the field located in the North sea. The horizontal grid of the full field model consists of $80 \times 100 \times 52$ grid cells with a resolution of 80×100 m. In this example, we have considered a sector model of this full field with top 18 producing layers and consists of 45×100 grid cells and it has around 20000 active grid cells.

Petro-elastic Modeling

For the calculation of seismic properties, we have used a pressure dependent petro-elastic model (PEM) for unconsolidated sand reservoir. Gassmann fluid substitution equation constitutes the main part of the rock physics modeling [2]. The seismic grid used here is same as the reservoir grid. This helps us running the coupled reservoir-seismic model smoothly without any up- or down-scaling between reservoir and

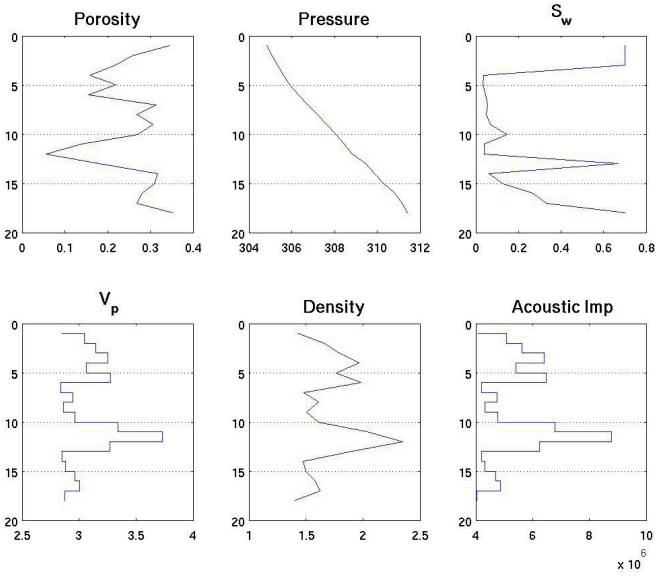

Figure 2: Rock physics template for a seismic trace

seismic grids. The seismic properties are calculated in every active grid cells. The Fig. 2 shows the rock physics template along one arbitrary seismic trace of the reservoir sector model. We can observe the effect of porosity and water saturation on the calculated $\mathbf{V}_P$ and acoustic impedance values along the trace. These values then become the inputs for the amplitude calculation based on 1D convolution.

Seismic Modeling by 1D Convolution

In order to calculate synthetic seismic gather, all saturated reservoir properties (e.g., $\mathbf{V}_P$, $\mathbf{V}_s$ calculated by PEM model and Gassmann equation) have been used along each trace in the depth direction. For our sector model with 45×100 grid cells in xy-direction, we have 4500 seismic traces along 18 layers. In order to calculate impedance contrast along each layer, we have used an average depth of the reservoir along each seismic trace. As already explained earlier, we have worked in depths while to perform wavelet sampling. In this case, the sampling of the wavelet is same as the sampling for seismic data. For each layer individually, we have used this wavelet for convolution with the calculated reflection coefficients. An example calculation of synthetic amplitude data for a single trace is shown in Fig 3. Here we have used Ricker wavelet with frequency of 25 Hz and the incidence angle is 5 degrees. For calculating 4D responses, we can compute amplitude data for both base and monitor surveys, and then take the difference between these two.

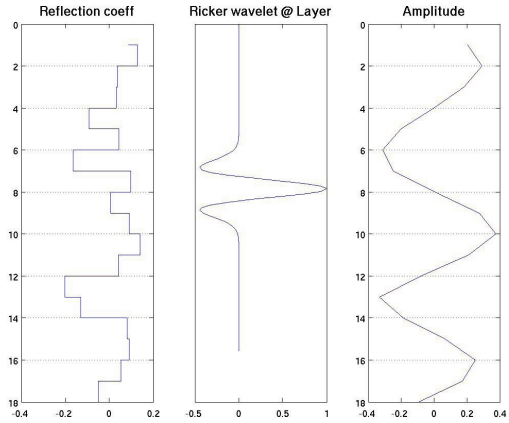

Figure 3: Seismic amplitude data along trace

Discussions & Comments

In this work, we have calculated synthetic seismic signatures of a sector model of a North sea reservoir. We have used the petro-elastic recipe as the basis of our rock physics modeling. The assumption of forward model linearity and log-Gaussian assumption of the prior models simplified the calculations. Also, we have used the wavelet sampling in depth, not in time. Thus, we have made several simplifications. More investigations are necessary to improve the overall quality of calculating synthetic seismograms.

Bibliography

[1] Aki K and Richards P, *Quantitative seismology*. W. H. Freeman & Co., 1980.

[2] Avseth P, Mukerji T, and Mavko G, *Qualitative seismic interpretation: Applying rock physics tools to reduce interpretation risk*. Cambridge University Press, 2005.

[3] Bachrach R, *Joint estimation of porosity and saturation using stochastic rock-physics modelling*, Geophysics, vol. 71, (2006).

[4] Batzle M, Wang Z, *Seismic properties of pore fluids*, Geophysics Prospecting, vol. 57, (1992).

[5] Bualnd A and Omre H, *Bayesian linearized AVO inversion*, Geophysics, Vol.68, No.1, (2003).

[6] Buland A, *Bayesian seismic AVO inversion*. PhD Thesis, Norwegian University of Science & Technology, 2002.

[7] Cerveny V, *Seismic ray theory*. Cambridge University Press, 2000.

[8] Dobrin M and Savit C, *Introduction to geophysical prospecting*. McGraw-Hill Companies, U.S.A., 1988.

[9] Gassmann F, *Uber die elastizitat poroser medien*, Vier. der Natur. Gesellschaft in Zurich, vol. 96, (1951).

[10] Ricker N, *The form and laws of propagation of seismic wavelets*, Geophysics, vol. 18, (1953).

[11] Saetrom J, *Hierarchical ensemble Kalman filter for observations of production and 4D seismic data*. Master's Thesis, Norwegian University of Science & Technology, 2007.

[12] Sen M, *Seismic inversion*. Society of Petroleum Engineers, U.S.A., 2006.

[13] Sheriff R and Geldart L , *Exploration seismology*. Cambridge University Press, 1999.

[14] Virieux J, *P-S wave propagation in heterogeneous media: Velocity-stress finite-difference method*, Geophysics, vol. 51, (1985).